

Multiple pre-edge structures in Cu *K*-edge x-ray absorption spectra of high- T_c cuprates revealed by high-resolution x-ray absorption spectroscopy

C. Gougoussis,¹ J.-P. Rueff,^{2,3} M. Calandra,¹ M. d'Astuto,¹ I. Jarrige,⁴ H. Ishii,⁵ A. Shukla,¹ I. Yamada,⁶ M. Azuma,⁷ and M. Takano⁶

¹CNRS and Institut de Minéralogie et de Physique des Milieux Condensés, case 115, 4 place Jussieu, 75252 Paris Cedex 05, France

²Synchrotron SOLEIL, L'Orme des Merisiers, Saint-Aubin, BP 48, 91192 Gif-sur-Yvette Cedex, France

³Laboratoire de Chimie Physique-Matière et Rayonnement, CNRS-UMR 7614, Université Pierre et Marie Curie, F-75005 Paris, France

⁴Synchrotron Radiation Research Unit, Japan Atomic Energy Agency, 1-1-1 Kouto, Sayo, Hyogo 679-5148, Japan

⁵National Synchrotron Radiation Research Center, Hsinchu 30076, Taiwan

⁶Department of Chemistry, Graduate School of Science and Engineering, Ehime University, 2-5 Bunkyo-Cho, Matsuyama, Ehime 790-8577, Japan

⁷Institute for Chemical Research, Kyoto University, Uji, Kyoto 611-0011, Japan

(Received 4 September 2009; revised manuscript received 26 May 2010; published 24 June 2010)

Using high-resolution x-ray absorption spectroscopy and state-of-the-art electronic structure calculations we demonstrate that the pre-edge region at the Cu *K* edge of high- T_c cuprates is composed of several excitations invisible in standard x-ray absorption spectra. We consider in detail the case of $\text{Ca}_{2-x}\text{CuO}_2\text{Cl}_2$ and show that the many pre-edge excitations (two for *c*-axis polarization, four for in-plane polarization and out-of-plane incident x-ray momentum) are dominated by off-site transitions and intersite hybridization. This demonstrates the relevance of approaches beyond the single-site model for the description of the pre edges of correlated materials. Finally, we show the occurrence of a doubling of the main edge peak that is most visible when the polarization is along the *c* axis. This doubling, that has not been seen in any previous absorption data in cuprates, is not reproduced by first-principles calculations. We suggest that this peak is due to many-body charge-transfer excitations while all the other visible far-edge structures are single particle in origin. Our work indicates that previous interpretations of the Cu *K*-edge x-ray absorption spectra in high- T_c cuprates can be profitably reconsidered.

DOI: [10.1103/PhysRevB.81.224519](https://doi.org/10.1103/PhysRevB.81.224519)

PACS number(s): 74.72.-h, 71.20.Be

I. INTRODUCTION

The interpretation of x-ray absorption spectroscopy (XAS) at the Cu *K* edge in high- T_c cuprates, and especially of the pre-edge features, remains a challenging issue due to the strongly correlated nature of these materials. Understanding the nature of the pre-edge features is relevant since these excitations are low in energy and probe the local environment of the absorbing atom. In several recent works¹⁻⁴ the presence of off-site excitations in transition-metal compounds such as NiO, cuprates, and cobaltates was demonstrated. Off-site excitations can occur by a direct transition of a 1*s* core electron to empty electronic states of the nearest-neighbor atoms.² This mechanism has a low intensity ($\sim 1\%$ of the edge jump) since the *p* states of the absorbing atoms are not involved. More frequently the off-site excitations are mediated by the on-site *p* states of the absorbing atom that are very extended and therefore hybridize with neighboring sites. When intersite excitations between 4*p*-Cu states of the absorbing atom and 3*d* states of a neighboring Cu atom occur, the information is very relevant since these features are typically weakly affected by core-hole attraction and thus they probe the excitation in the absence of a core hole in the final state. In some cases off-site transitions can be used to measure the charge-transfer gap, as was recently suggested for NiO.² Therefore, a full understanding of pre-edge features and of their possible nonlocal nature leads to the knowledge of the hybridization mechanism between different orbitals in the low-energy region (up to some electron

volt from the Fermi level) and of the position of the upper Hubbard band in the absence of a core hole in the final state.²

In the case of high- T_c cuprates, and of correlated materials in general, the occurrence of many-body charge-transfer excitations in the edge region has been widely debated.⁵⁻⁷ Recently, using first-principles calculations, we suggested⁸ that edge and far-edge structures previously attributed to charge-transfer effects were actually single particle in origin. Thus most of the multideterminant effects seen in photoemission seem to be suppressed in absorption, probably by the presence of a final state in the XAS cross-section.

In this work we present high-resolution angular-resolved partial-fluorescence yield (PFY) x-ray absorption measurements and first-principles electronic structure calculations of the recently synthesized $\text{Ca}_{2-x}\text{CuO}_2\text{Cl}_2$ oxychlorides.⁹ These materials form a new family of high- T_c superconductors with a critical temperature peaking at 43 K at optimal nominal doping level (after postannealing). The oxychlorides are appropriate for investigating the electronic properties of the CuO_2 plane. They are, for example, well suited for calculations because of lesser structural disorder and the absence of rare-earth atoms. They also present peculiar features compared to the cuprates such as a checkerboard pattern of charge inhomogeneities^{10,11} at odds with the stripes in the cuprates. High-resolution XAS allows us to identify new pre-edge electronic excitations and a doubling of the main edge that are not visible in previous XAS measurements in high- T_c cuprates. Importantly we find that most of these excitations are single particle in nature. After identifying the

single-particle excitations and addressing the role of many-body charge-transfer effects in the XAS spectra, we come to the conclusion that the interpretation of Cu K -edge XAS in cuprates should be revisited.

Section II presents the experimental and theoretical details and draws a comparison between the measured PFY-XAS spectra of $\text{Ca}_{1.8}\text{CuO}_2\text{Cl}_2$ and of La_2CuO_4 . In Sec. III, we confront the experimental data with the calculated cross-section and identify the single-particle peaks using the projected density of states on selected electronic states in the presence of a core hole in the $1s$ state. Finally we discuss the relevance of our results for the understanding of the empty-state electronic structure in high- T_c cuprates.

II. TECHNICAL DETAILS

A. Experiment

The experiment was carried out at SPring-8 on the inelastic x-ray scattering (IXS) beamline BL12XU. The incident energy was selected by a Si(111) double crystal coupled to a high-resolution four-bounce Si(400) monochromator providing an estimated bandwidth of 220 meV. We have used well-characterized superconducting single crystals of $\text{Ca}_{2-x}\text{CuO}_2\text{Cl}_2$ ($x=0.2$).⁹ To prevent degradation of the samples known to be highly hygroscopic, the crystals were covered with a grease suitable for low-temperature measurements. The superconducting temperature of 35 K measured by superconducting quantum interference device confirms that the intrinsic quality was preserved. The sample orientation was verified by x-ray diffraction prior to measurements.

The absorption spectra were recorded in the PFY mode using the beamline IXS spectrometer. The PFY-XAS consists of measuring the intensity variations in the Cu $K\alpha$ ($2p \rightarrow 1s$) emission line while scanning the incident energy through the Cu K edge. With respect to conventional XAS, the PFY method yields an improved intrinsic resolution as the lifetime broadening effect in the PFY final state (with a $2p$ core hole) is considerably smaller than that of standard XAS at the K edge (with a $1s$ core hole). The spectrometer was equipped with a 2 m bending radius Si(444) analyzer working at Bragg angle of 79.3° at the Cu $K\alpha$ energy (8048 eV) and a high-flux silicon drift detector. The total-energy resolution was estimated at 250 meV from the width of the elastic line. The sample was mounted on a goniometer head with the c axis (normal to the surface) in the horizontal plane. The PFY absorption spectra were acquired with the polarization of the incident photons set either parallel or perpendicular to the c axis upon rotating the sample around a vertical axis. The spectra were corrected for self-absorption effect using the FLUO code developed by D. Haskel (Advanced Photon Source, Argonne).

B. Calculation

Ab initio calculations on $\text{Ca}_{2-x}\text{CuO}_2\text{Cl}_2$ are performed using spin-polarized density-functional theory (DFT) with PBE exchange correlation.¹² We cross-check our results with the DFT+ U approximation with $U=9.6$ eV as used in other cuprates.⁸ The calculation is performed with the XSPECTRA

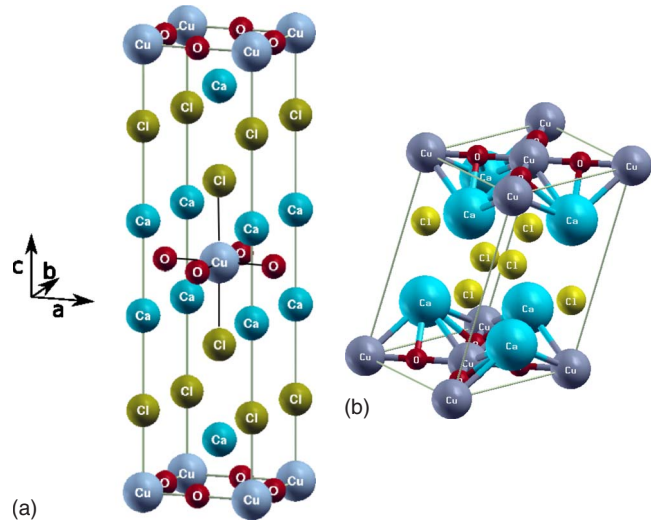


FIG. 1. (Color online) Left: crystal structure of $\text{Ca}_{2-x}\text{CuO}_2\text{Cl}_2$ (Ref. 17). Right: 14 atoms monoclinic supercell used in the calculation.

code^{8,13} available under the GPL license in the QUANTUM-ESPRESSO package.¹⁴ We use ultrasoft pseudopotentials¹⁵ for all atomic species. The $1s$ core hole is included in the pseudopotential of the absorbing atom. For the Cu pseudopotential we use nonlinear core corrections¹⁶ and do not include semicore states. It has been shown⁸ that the inclusion of the copper semicore states in the valence states is not necessary for an accurate description of XAS in cuprates.

For the XAS calculation we use a monoclinic supercell containing one CuO plane and 14 atoms with experimental lattice parameters⁹ (see Fig. 1). The magnetic state of $\text{Ca}_2\text{CuO}_2\text{Cl}_2$ has not been yet resolved, but for simplicity we assume a collinear antiferromagnetism, similar to other cuprates.

The wave functions are expanded on a plane-wave basis with a 30 Ry cutoff for the wave functions and 400 Ry for the charge density. A uniform Monkhorst-Pack $6 \times 6 \times 2$ k -points grid (with respect to the antiferromagnetic unit cell) is used for the charge-density calculation with a Methfessel-Paxton smearing of 0.05 Ry. The hole doping is treated by adding a compensating charge background, leading at $x=0.2$ to a nonmagnetic state in agreement with experiments.

The XAS cross-section is calculated in the dipole approximation using an ultrasoft-based continued fraction approach⁸ and projector augmented wave (PAW) reconstruction.¹⁸ Two PAW projectors are used in the absorbing atom pseudopotential. A uniform shifted $6 \times 6 \times 6$ k -point grid is used for the continued fraction calculation. A 0.3 eV Lorentzian convolution, gradually increasing to 1.5 eV after the edge is used to match the experimental width.

III. RESULTS

A. Experiment

In Fig. 2 we show the measured PFY-XAS data at the Cu K edge in $\text{Ca}_{2-x}\text{CuO}_2\text{Cl}_2$ compared to previous PFY-XAS measurements¹ on La_2CuO_4 . In the case of $\text{Ca}_{2-x}\text{CuO}_2\text{Cl}_2$ the

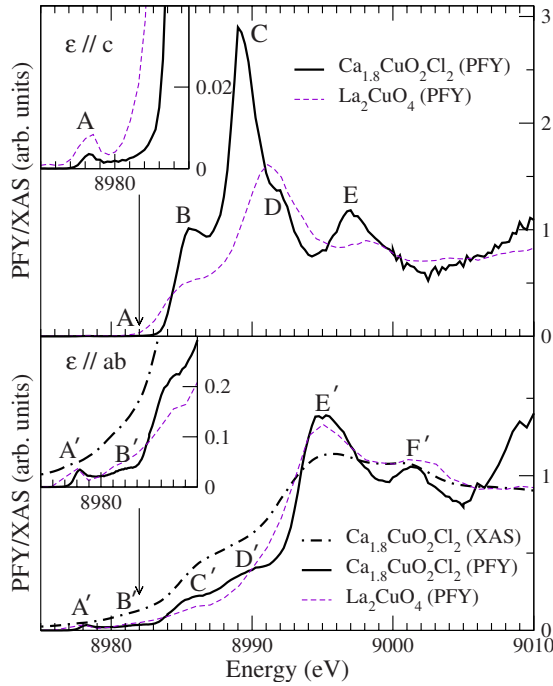


FIG. 2. (Color online) Comparison between the PFY-XAS Cu K-edge spectra of $\text{Ca}_{2-x}\text{CuO}_2\text{Cl}_2$ (solid lines) and La_2CuO_4 (dashed lines) for polarizations $\epsilon \parallel c$ and $\epsilon \parallel ab$, respectively, in the top and the bottom panels. In the case of $\text{Ca}_{2-x}\text{CuO}_2\text{Cl}_2$ the scattering geometries considered are: (i) \mathbf{k} parallel to the ab plane and ϵ parallel to the c axis, labeled shortly $\epsilon \parallel c$ and (ii) \mathbf{k} parallel to the c axis and ϵ parallel to the ab plane, labeled $\epsilon \parallel ab$. In the case of La_2CuO_4 the geometries are slightly different, as reported in Ref. 1.

scattering geometries considered are: (i) \mathbf{k} parallel to the ab plane and ϵ parallel to the c axis, labeled shortly $\epsilon \parallel c$ and (ii) \mathbf{k} parallel to the c axis and ϵ parallel to the ab plane, labeled $\epsilon \parallel ab$. In the case of La_2CuO_4 the geometries are slightly different, as reported in Ref. 1. For the $\epsilon \parallel ab$ geometry we also plot standard XAS data in Fig. 2.

In the absence of a core hole all d states are filled except the $3d_{x^2-y^2}$ orbital which is half empty. However, the $3d_{x^2-y^2}$ being planar, the quadrupolar part is forbidden in both geometries. This is due to the fact that the quadrupolar matrix element of the absorption cross-section includes a term $(\mathbf{k} \cdot \mathbf{r})(\epsilon \cdot \mathbf{r})$. In the $\epsilon \parallel c$ geometry $\epsilon \cdot \mathbf{r} = 0$ while in the $\epsilon \parallel ab$ geometry $\mathbf{k} \cdot \mathbf{r} = 0$. So in both experimental settings the matrix element is zero.

We first focus on the pre-edge region. At 8978 eV in $\epsilon \parallel c$ geometry an extremely small feature (labeled A in the following) is present, its intensity is 0.4% of the edge jump. A similar feature is present at the same energy in the $\epsilon \parallel ab$ geometry (labeled A'), however, the intensity in this direction is substantially larger, on the order of 3% of the edge jump. Interestingly this feature in the $\epsilon \parallel ab$ geometry merges with a second broader band centered at 8982 eV (labeled B'). Given the weakness of some of these excitations, particularly along the c axis, we reconsider our published PFY-XAS Cu-K-edge La_2CuO_4 data to see if similar features occur.¹ This is indeed the case, however, these small features (in both geometries) were not discussed in our previous work.¹ We have not found any XAS measurements^{5,7,19-21} on

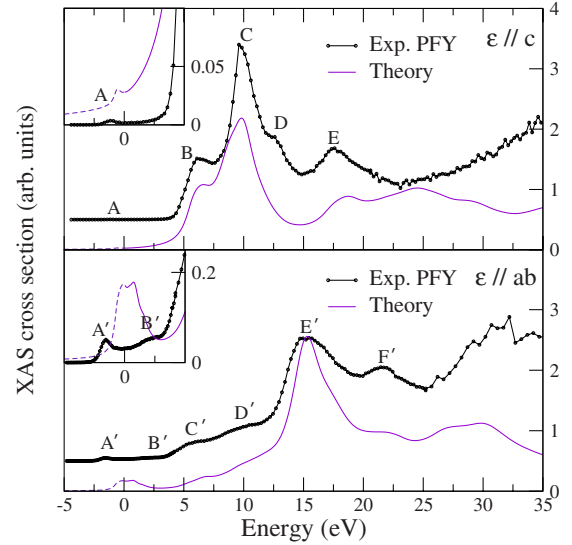


FIG. 3. (Color online) Comparison between calculated Cu K-edge XAS (solid lines) and experimental (dots) PFY-XAS of $\text{Ca}_{2-x}\text{CuO}_2\text{Cl}_2$ ($x=0.2$) for both conditions of polarization $\epsilon \parallel c$ and $\epsilon \parallel ab$, respectively, in the top and the bottom panels. The core-hole width of the calculation is 0.7 eV. The zero energy corresponds to 8979.2 eV

cuprates displaying the A and A' features. We also performed XAS measurements on the most interesting $\epsilon \parallel ab$ direction and found that the standard XAS spectrum shows a very broad tail extending down to the pre-edge region. None of the pre-edge features that are clearly resolved by PFY are visible here, as in the case of La_2CuO_4 . Furthermore the B' at 8922 eV in the $\epsilon \parallel ab$ geometry is usually assumed to be completely quadrupolar. This is due to the lesser sensitivity of standard XAS data when compared with PFY measurements.

In $\text{Ca}_{2-x}\text{CuO}_2\text{Cl}_2$ the first feature is probably not more than 0.3 eV above the Fermi level and thus it is relevant for its low-energy physics. The other pre-edge features at higher energies (labeled B, B', and C' in Fig. 3) are common to those of other cuprates.

The structure in the absorption edge is similar in the two systems, apart from a remarkable difference. In the case of $\text{Ca}_{2-x}\text{CuO}_2\text{Cl}_2$ with $\epsilon \parallel c$ geometry the edge (peak of the whiteline) at 8989 eV is accompanied by a distinct shoulder at 8992 eV. In $\text{Ca}_{2-x}\text{CuO}_2\text{Cl}_2$ for $\epsilon \parallel ab$ the edge seems substantially larger than the experimental resolution, suggesting the presence of a second peak in this case too. In La_2CuO_4 there is no evidence of such a splitting. However the poorer experimental resolution we had in Ref. 1 could hinder the detection of a second peak. Consequently higher resolution measurements are necessary to clarify if this splitting is a general feature of high- T_c cuprates.

B. Theoretical understanding

1. Pre-edge region

To understand the origin of the features seen in the absorption spectra, we carried out extensive DFT calculations

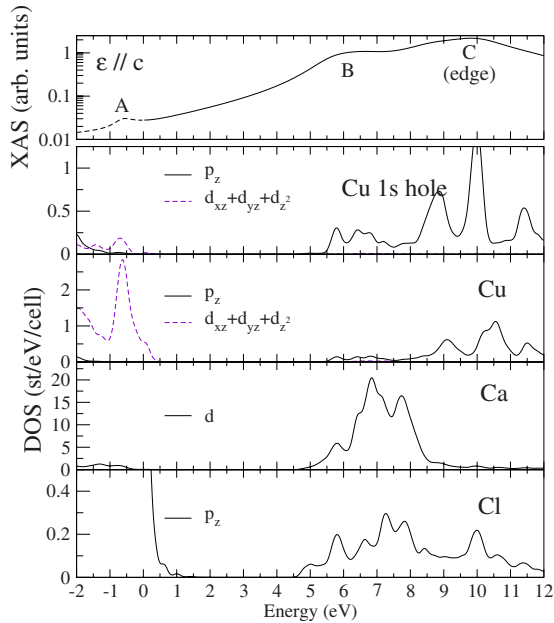


FIG. 4. (Color online) Comparison between the calculated XAS cross-section with ϵ in the c direction and the density of states in the presence of a core hole projected on selected orbitals. Note that in the top panel of this figure the XAS has been plotted in log scale to enhance the low-intensity low-energy peaks.

for $\text{Ca}_{2-x}\text{CuO}_2\text{Cl}_2$. In the presence of a core hole the $d_{x^2-y^2}$ state around the absorbing atom is the only d state partially occupied. In the pre-edge region the situation is complicated by the fact that the system is metallic and it is hard to isolate the occupied states from the unoccupied ones, even as far as the dipolar part is concerned. As a consequence we have decided to shift the Fermi level 0.7 eV below that found in the supercell calculation (this is illustrated by the dashed line in Figs. 3–5). This shift improves the agreement with experiments in the low-energy region. However the drawback is that a small tail of the $d_{xz}+d_{yz}+d_{z^2}$ projected density of states becomes unoccupied generating a quadrupolar term (see Fig. 4). By direct calculation of the XAS quadrupolar cross-section we have verified that this quadrupolar term is completely negligible with respect to the dipolar part emerging from the Fermi-level downshift. Despite these difficulties and the strongly correlated nature of the system which is a real challenge for density-functional theory, we find good overall agreement with experiments.

In the pre-edge region and $\epsilon||c$ geometry, we reproduce the low-intensity peak A as it can be seen in Fig. 3. The analysis based on the density of states projected on selected orbitals in the presence of a core hole in the final state (Fig. 4) suggests that the peak is essentially due to an off-site transition to Cl $2p_z$ states and practically negligible quadrupolar component. This is analogous to what was found in NiO ,² namely, a very low-energy dipolar feature due to direct off-site transition to nearby atoms. The situation is not as favorable in the $\epsilon||ab$ geometry where the broadband B' and the small feature A' are replaced in our calculation by a more intense broadband (Figs. 3 and 5). This disagreement is a reminder that DFT has limitations when it comes to the description of the low-energy physics of high- T_c compounds.

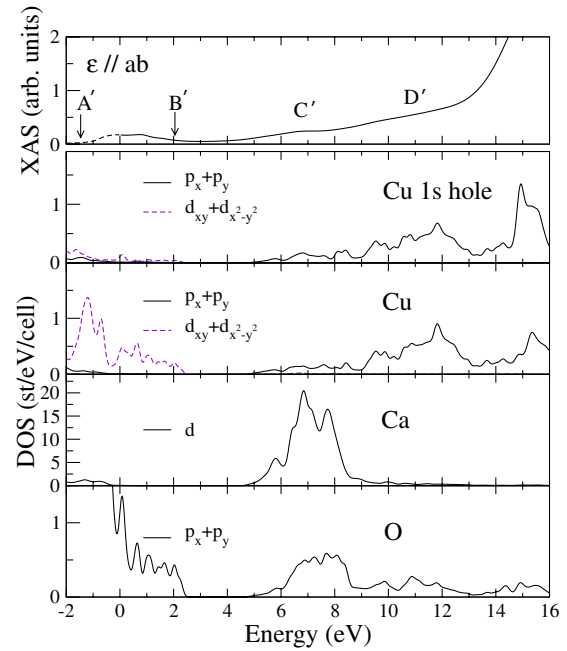


FIG. 5. (Color online) Comparison between the calculated XAS cross-section with ϵ in the CuO plane direction and the density of states in the presence of a core hole projected on selected orbitals.

On the other hand, the peaks C' and D' are correctly reproduced. The C' peak is due to intersite hybridization between Cu $4p$, O $2p_{xy}$, and Ca d states while the D' peak is due to transitions to on-site Cu $4p$ states. Similarly to the C' peak, the B peak in $\epsilon||c$ geometry is due to intersite Cu $4p$, Ca d , and Cl p_z states. Thus all the pre-edge peaks A, B, and C' are dominated by off-site transitions.

2. Edge-to-far-edge region

This energy region has been studied in detail in the past mainly due to the work of Tolentino *et al.*⁵ and Kosugi *et al.*⁷ suggesting that multideterminant excitations could occur. In particular, in Ref. 5 it was proposed that the edge peaks C and E' are due to transition to $|3d^{10}\bar{L}\rangle$ states while their supposed satellites, E and F' are due to $|3d^9\bar{L}\rangle$. The original proposal was on Cu K edge of La_2CuO_4 . However in Ref. 8 we showed that this system is not well described by DFT in this region due to the difficulty in treating La f states. Nevertheless we concluded in Ref. 8 that apart from a shift of the E peak to high energy, generated by an incorrect treatment of La f states in DFT, C, E, E', and F' were most likely due to single-particle excitations. The present compound is ideal to verify this conclusion since no rare earths are present. Indeed we find that peaks C, E, E', and F' are correctly reproduced confirming their single-particle nature.

In the $\epsilon||c$ direction a peak labeled D is found. This peak is absent from our single-particle calculation. This suggests that multideterminant charge-transfer effects could indeed occur in cuprates. In order to test our conjecture one should consider the convolution between hard x-ray Cu $1s$ photoemission data and first-principles calculations. This procedure should give semiquantitative agreement with the Cu K -edge XAS.^{22–26} The difficulty in the present case is that

there are no photoemission data for this system so measurements and calculations on other correlated compounds are needed.

IV. CONCLUSION

In this work we have carried out Cu *K*-edge PFY-XAS measurements and state-of-the-art first-principles calculations in high- T_c cuprates $\text{Ca}_{2-x}\text{CuO}_2\text{Cl}_2$. We have shown that rich structure due to dipolar transitions occurs in the pre-edge region. By performing electronic structure calculations we have shown that pre-edge peaks are dominated by off-site transitions. Furthermore we have shown the occurrence of new excitations in the low-energy region, at less than 0.5 eV from the Fermi level. In this energy region DFT calculations only partially capture the relevant physics of the system since they fail in describing the in-plane excitations. Our work demonstrates the need of going beyond single-site cluster models and, for what concerns correlation effects, beyond density-functional theory, in order to explain Cu *K*-edge XAS of cuprates.

Previous work⁵⁻⁷ invokes a strong influence of many-body effects to explain the features observed in XAS *K*-edge

spectra of high- T_c materials. Notably the invocation of a correlated ground state and the rearrangement of the energy states due to the core-hole effect have lead earlier authors to conclude that some of the most prominent peaks in XAS spectra are not due to single-particle excitations. This interpretation is also inspired from core-level photoemission data but here we show that the situation is not analogous and that much of the XAS *K*-edge spectrum can, in fact, be explained invoking single-particle excitations. Further, we find that many-body effects due to charge transfer do occur but in a different way from earlier interpretations.

The ramifications of this reinterpretation go beyond XAS spectroscopy. It will suffice to note that RIXS spectra use the resonances found in XAS to excite particular intermediate states.

ACKNOWLEDGMENTS

Calculations were performed at the IDRIS supercomputing center (Project No. 081202). M.C. and C.G. acknowledge fruitful discussions with F. Mauri, Ch. Brouder, and Ph. Sainctavit.

-
- ¹A. Shukla, M. Calandra, M. Taguchi, A. Kotani, G. Vanko, and S.-W. Cheong, *Phys. Rev. Lett.* **96**, 077006 (2006).
- ²C. Gougoussis, M. Calandra, A. Seitsonen, Ch. Brouder, A. Shukla, and F. Mauri, *Phys. Rev. B* **79**, 045118 (2009).
- ³A. Kotani, K. Okada, G. Vanko, G. Dhalenne, A. Revcolevschi, P. Giura, and A. Shukla, *Phys. Rev. B* **77**, 205116 (2008).
- ⁴G. Vankó, F. de Groot, S. Huotari, R. Cava, T. Lorenz, and M. Reuther, [arXiv:0802.2744](https://arxiv.org/abs/0802.2744) (unpublished).
- ⁵H. Tolentino, M. Medarde, A. Fontaine, F. Baudelet, E. Dartyge, D. Guay, and G. Tourillon, *Phys. Rev. B* **45**, 8091 (1992).
- ⁶R. Bair and W. Goddard, *Phys. Rev. B* **22**, 2767 (1980).
- ⁷N. Kosugi, Y. Tokura, H. Takagi, and S. Uchida, *Phys. Rev. B* **41**, 131 (1990).
- ⁸C. Gougoussis, M. Calandra, A. P. Seitsonen, and F. Mauri, *Phys. Rev. B* **80**, 075102 (2009).
- ⁹I. Yamada, A. A. Belik, M. Azuma, S. Harjo, T. Kamiyama, Y. Shimakawa, and M. Takano, *Phys. Rev. B* **72**, 224503 (2005); I. Yamada, M. Azumaa, Y. Shimakawaa, and M. Takano, *Physica C* **460-462**, 420 (2007).
- ¹⁰Z. Hiroi, N. Kobayashi, and M. Takano, *Nature (London)* **371**, 139 (1994).
- ¹¹T. Hanaguri, C. Lupien, Y. Kohsaka, D.-H. Lee, M. Azuma, M. Takano, H. Takagi, and J. C. Davis, *Nature (London)* **430**, 1001 (2004).
- ¹²J. P. Perdew, K. Burke, and M. Ernzerhof, *Phys. Rev. Lett.* **77**, 3865 (1996).
- ¹³The XSPECTRA code by C. Gougoussis, M. Calandra, A. Seitsonen, and F. Mauri is distributed under the gnu license in the current CVS version of the QUANTUM-ESPRESSO code.
- ¹⁴P. Giannozzi, S. Baroni, N. Bonini, M. Calandra, R. Car, C. Cavazzoni, D. Ceresoli, G. L. Chiarotti, M. Cococcioni, I. Dabo, A. Dal Corso, S. de Gironcoli, S. Fabris, G. Fratesi, R. Gebauer, U. Gerstmann, C. Gougoussis, A. Kokalj, M. Lazzeri, L. Martin-Samos, N. Marzari, F. Mauri, R. Mazzarello, S. Paolini, A. Pasquarello, L. Paulatto, C. Sbraccia, S. Scandolo, G. Sclauzero, A. P. Seitsonen, A. Smogunov, P. Umari, and R. M. Wentzcovitch, *J. Phys.: Condens. Matter* **21**, 395502 (2009).
- ¹⁵D. Vanderbilt, *Phys. Rev. B* **41**, 7892 (1990).
- ¹⁶S. G. Louie, S. Froyen, and M. L. Cohen, *Phys. Rev. B* **26**, 1738 (1982).
- ¹⁷A. Kokalj, *Comput. Mater. Sci.* **28**, 155 (2003).
- ¹⁸P. E. Blöchl, *Phys. Rev. B* **50**, 17953 (1994).
- ¹⁹See, for example, experimental Cu *1s* hard x-ray photoemission collected at the Hiroshima Synchrotron radiation center at <http://www.hsrc.hiroshima-u.ac.jp/cuprates.htm>
- ²⁰J. M. Tranquada, S. M. Heald, and A. R. Moodenbaugh, *Phys. Rev. B* **36**, 5263 (1987).
- ²¹J. M. Tranquada, S. M. Heald, W. Kunmann, A. R. Moodenbaugh, S. L. Qiu, Y. Xu, and P. K. Davies, *Phys. Rev. B* **44**, 5176 (1991).
- ²²P. Nozières and C. T. De Dominicis, *Phys. Rev.* **178**, 1097 (1969).
- ²³D. Malterre, *Phys. Rev. B* **43**, 1391 (1991).
- ²⁴G. D. Mahan, *Solid State Phys.* **29**, 75 (1994).
- ²⁵O. Gunnarsson and K. Schönhammer, *Phys. Rev. B* **31**, 4815 (1985).
- ²⁶Y. Hammoud, J. C. Parlebas, and F. Gautier, *J. Phys. F: Met. Phys.* **17**, 503 (1987).